6th AIAA Flow Control Conference
25 - 28 June 2012, New Orleans, Louisiana

AIAA 2012-2809

Experimental Study and Plasma Control of an Unstarting Supersonic Flow

[*]Seong-kyun Im[1], [§]Hyungrok Do[2], [*][Π]M. Godfrey Mungal[3] and [*]Mark A. Cappelli[4]
[*]*Mechanical Engineering Department, Stanford University, Stanford, California, 94305*
[§]*Department of Aerospace and Mechanical Engineering, University of Notre Dame, Notre Dame, Indiana, 46556*
[Π]*School of Engineering, Santa Clara University, Santa Clara, California, 95053*

The unstart induced by a transverse jet in a Mach 4.7 model inlet flow is visualized by planar laser scattering from condensed CO_2 particles at low freestream static pressure (1kPa) and temperature (60K) for various boundary layer conditions. We find that the formation of an unstart shock is initiated on the relatively thick boundary layer side and its structure depends on the boundary layer conditions. The pseudo-shock or oblique shocks that precede unstart propagate upstream in symmetric and asymmetric boundary layer conditions, respectively. It is found that the pseudo-shock has a quasi-stationary mode resulting in longer overall unstart events. The results suggest that the unstart process can be influenced and possibly delayed by the control of the boundary layer conditions. In this paper, we present preliminary results on boundary layer manipulation of an unstarting supersonic flow using Dielectric Barrier Discharge (DBD) actuation. We find that the asymmetric boundary layer condition that generally leads to the formation and propagation of an oblique unstart shock, when actuated, can be transformed the flow to resemble that of a symmetric condition which leads to the generation of a pseudo-shock, extending the unstart duration by 22 %.

I. Introduction

Ustart, a condition that can cause in-flight scramjet engine malfunction has been described in several prior studies.[1-6] It is believed that the thermal choking that results from the heat release in the combustor is the cause of this phenomenon.[7-8] A pressure rise followed by thermal choking leads to boundary layer separation and growth that reduces the core internal flow area and forces the flow into a subsonic regime. This cascades into disturbances and blockage of the upstream flow.[9-10] It is difficult to reproduce combustion-driven unstart in ground test facilities as it requires high enthalpy supersonic flows of relatively long test duration. However, the physics of unstart phenomena can be investigated by partially reproducing flight conditions. For example, Wagner et al.[11] studied the formation and dynamics of unstart in a ground test facility that mimics the thermal choking by the movement of a mechanical flap which produces flow blockage at flight Mach numbers and pressures but at low temperature. In a similar model inlet flow, Do et al.[12-13] studied unstart as a result of flow blockage generated by downstream mass injection. In the studies of Do et al[12-13], it was found that the boundary layer characteristics and separation strongly affect the unstart process, indicating that boundary layer control in a supersonic inlet duct can be used to delay or even possibly avoid unstart. Studies of unstart delay through the use of isolators[14-15] and boundary layer bleeding[8] have been previously reported. In this paper, we report on first results on the use of dielectric barrier discharge (DBD) actuation of boundary layers for supersonic inlet flow unstart control.

There has been a growth in research activity on the use of DBD actuators in aerodynamic flow applications such as boundary layer reattachment,[16-19] boundary layer transition delay,[20] turbulent boundary layer manipulation[21-22] and vortex generation[23] since the idea was first introduced by Roth et al.[24] A dielectric barrier discharge (DBD) actuator consists of flow-exposed and dielectric embedded electrodes driven by alternating current (AC). An asymmetric configuration is designed to impose a force on the ionized gas generated by the discharge and to induce a directional

[1] Graduate Student, AIAA Student Member.
[2] Assistant Professor.
[3] Professor. AIAA Associate Fellow.
[4] Professor.

flow of neutral gas through collisions with the drifting ions. Several researchers have developed models and simulations of actuator performance.[25] However, most of the previous studies have been performed in subsonic flow regimes. In contrast, there have been very few studies of the use of DBD actuators for the control of supersonic flows.[26] Most supersonic flow control studies that engage plasmas generally employ relatively high power direct current discharges.[27-28] In this paper, we present the actuation of supersonic model inlet flows with low power DBD actuators through spanwise forcing. The spanwise forcing thins the boundary layer and leads to a noticeable change in the unstart shock structure and in unstart delay.

In our studies, important flow features (e.g. boundary layers, slip lines, shock waves, and shock-wave boundary-layer interactions (SWBLI)) are visualized by Planar Laser Rayleigh Scattering (PLRS) of a laser light sheet from condensed CO_2 particles. This diagnostic technique was first proposed by Miles and colleagues[29-30] as a flow visualization method that is suitable for use in low temperature and low pressure supersonic flows expanded through the diverging section of converging/diverging nozzles. Gaseous CO_2 condensed by the sudden temperature drop during expansion and acceleration form nanometer-size particles which serve as markers of flow structure through scattered laser light. These CO_2 particles sublime in flow regions where the static temperature increases (e.g., within boundary layers or following strong shocks), and so the boundaries between these regions are discerned with high fidelity and contrast. This PLRS visualization enables us to observe these flow features under unstart flow conditions.

II. Experimental Setup

The experimental facility consists of a supersonic tunnel, a laser diagnostic system, and a longitudinal DBD actuator pair fabricated into the wall of a model inlet-duct (integrated into the tunnel) in which air is injected through one wall, as shown schematically in Fig. 1. A typical in-draft blow-down wind tunnel driven by a two-dimensional converging/diverging nozzle (25:1 area ratio) is used to produce the supersonic flow. The freestream Mach number (Ma = 4.7 ± 0.2) of the base flow in the test section is determined by measuring the incident/reflected shock angle on a test wedge and is independently confirmed by PIV measurements assuming the theoretical static temperature (Ts = 60 ± 4 K). A high pressure air/CO_2 mixture (P_0 = 350 kPa and T_0 = 300 K, 3:1 volume ratio) expands into the 40 mm by 40 mm cross sectional area tunnel test section. The useful test time is approximately 3 seconds. The static pressure is about 1 kPa. Optical access is provided by windows placed on both sides of the test section. Static pressure traces on the bottom wall of the tunnel are recorded using a fast response pressure sensor (PCB Piezotronics, Model 113B26). This pressure trace will be used to determine the time to reach unstart after mass injection (discussed below).

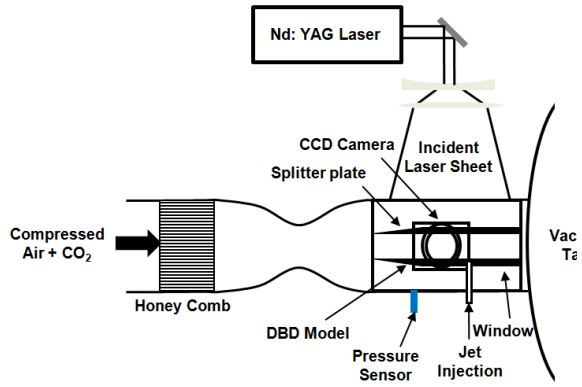

Figure 1. Schematic of experimental setup.

The model inlet-duct is defined by one or two 3 mm thick 12° wedged flat splitter plates (two are shown in Fig. 1) that span the 40 mm width of the tunnel for desired flow conditions. For asymmetric boundary layer conditions in which the model inlet flow has a thick turbulent boundary layer, one splitter plate is used to divide the test section into two regions with equal cross-sectional area. This splitter plate has a transparent plexiglass window for optical access to the region below. For symmetric boundary layer conditions and the generation of thin boundary layers, two plates (as shown in the figure) are used to isolate the model inlet flow from the thick boundary layers on the upper and lower tunnel wall. The height of the model inlet is 18.5 mm in all cases, except for the plasma control studies, where a height of 15 mm is used. Five flow configurations are studied overall to investigate the influence of boundary layer conditions on unstart. These five configurations are shown in Fig. 2, and defined as Cases I - V. In Cases I to IV, a single splitter plate is used to configure the model inlet flow. For case I, the transverse jet is injected into a relatively thick boundary layer (tunnel lower wall boundary layer) through a 3 mm diameter hole located 75 mm from the tip of the splitter plate The boundary layer on the upper surface of this model inlet (on the lower side of the splitter plate) grows naturally from the leading edge of the plate. For Case II, the splitter plate launches an oblique shock into this model inlet flow test section. In this case, the jet is injected through the splitter plate with the jet fluid delivered via a tube that traverses the lower half of the tunnel. The jet injection is now delivered into a

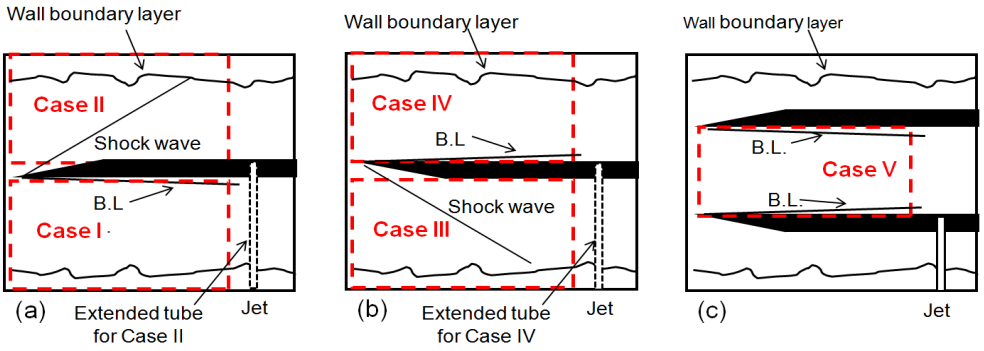

Figure 2. Schematics of flow configurations: (a) Case I and II, (b) Case III and IV, and (c) Case V.

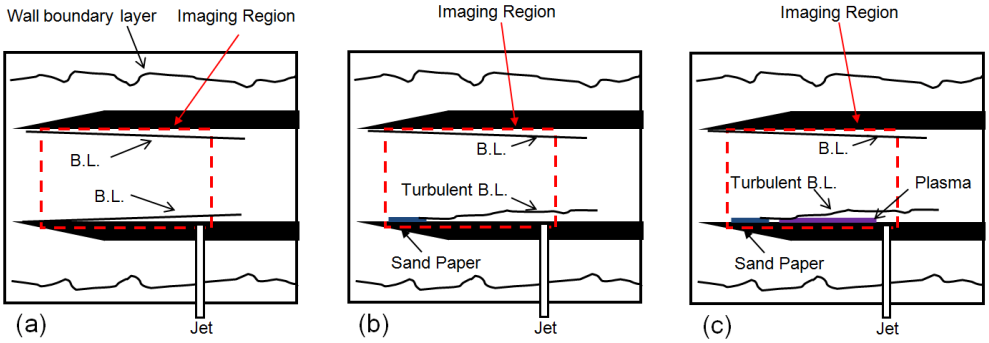

Figure 3. Schematics of flow configurations: (a) Case VI, (b) Case VII, and (c) Case VIII.

relatively thin boundary layer that originates from the splitter plate tip. Case II also has relatively thick boundary layer along the upper wall. Cases III and IV are similar to Cases I and II, but the splitter plate is flipped along the vertical direction and now launches the shock wave into the lower half of test section. All four cases are considered to be "asymmetric" inlet flow conditions, as each involves the presence of a very thick (and turbulent) boundary layer along that portion of the inlet model defined by the tunnel wall. Case V introduces a second splitter plate that can isolate the inlet model flow from this tunnel wall boundary layer. In this case, both boundary layers grow naturally from the leading edge of each plate with the jet injected through one. Case V is considered to be a "symmetric" inlet flow condition.

While we describe here, the unstart dynamics seen in all five configurations, three additional flow configurations are considered for plasma actuation studies, with Case V as a starting point, as depicted in Fig. 3. In the first of these configurations (Case VI), boundary layers grow naturally from the leading edge of each plate. This configuration is the same as that of Case V, except the model inlet height defined by the splitter plate separation is 15 mm. For Case VII and VIII, sand paper (120 Grit, 40 mm wide and 20 mm long) is attached to the bottom plate starting 10 mm downstream from the leading edge (to just upstream of the DBD) to trip the otherwise laminar boundary layer, creating a relatively thick turbulent boundary. The DBD actuator is only activated in the Case VIII flow configuration. The upper plate is fabricated from polycarbonate to enable laser access. A DBD actuator is integrated into the upper surface of the lower plate. A portion of the plate that accommodates the DBD actuator was cast from acrylic, with an epoxy (Loctite Hysol 1C) serving as a dielectric layer (approximately 2 mm thick) isolating the buried electrode from the top exposed electrode and discharge. Both electrodes consist of a single copper metal strip, oriented parallel to the flow (streamwise direction). The exposed and buried electrodes (0.1 mm thick) are 75 mm in length and 7 mm wide, and 75 mm in length and 25 mm wide, respectively. The exposed electrode is centered over the buried electrode, and both electrodes are placed along the center of the model with the leading edge of the electrodes located 40

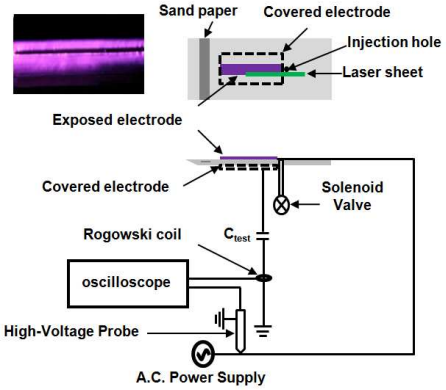

Figure 4. DBD actuator model.

mm downstream from the model inlet lip. A 3 mm diameter hole is located at the end of the DBD actuator, 118 mm downstream of the leading edge, to introduce an air jet which serves as a means of injecting mass into the supersonic inlet flow. As shown in Fig. 4, the laser sheet (500 μm thickness) illuminates a region of the flow for visualization. An AC power supply (GBS Elektronik GmbH, Minipuls 6) is used to drive the surface DBD discharge. A Rogowski coil (Pearson Electronics, Model 2877) and a 1000:1 high voltage probe (Tektronix, P6015A) are used to record current and voltage traces, respectively. The DBD actuator is driven at 20 kHz (with the buried electrode grounded) and a 6 kV peak to peak voltage. A typical image of its emission (viewed from above) while exposed to the Ma = 4.7 flow taken by a digital camera with a 1/30 second exposure time is presented as the inset to Fig. 4.

A Nd:YAG laser (New wave, Gemini PIV, 100mJ/pulse energy, 10Hz, 532nm) is shaped into a thin sheet using two cylindrical lenses (f = 200mm) and a convex spherical lens (f= 250mm), and directed into the test section for the PLRS diagnostic. A CCD camera (La Vision, Imager Intense, 1376 by 1040 pixel array) detects the scattered light at 90 degrees to the plane of the laser sheet. Laser firing for the PLRS is synchronized to the CCD camera exposure (3 μs). Phase-locking is used to investigate phase dependency on the DBD actuation. Laser firing is triggered by the rise in discharge voltage as obtained using a high voltage probe on the powered lead, and is delayed to acquire images at different phases using a pulse delay generator (SRS, DG 535). Note that the images shown (when the plasma is active) are phase delayed to depict the flow when actuation is strongest. In all of the experiments, an output reference from the laser Q-switch is used to trigger the jet injection and is delayed as desired by a pulse delay generator (SRS, DG 535). The mass injection is controlled by a solenoid valve (ASCO, Red Hat II) driven by a controller (Optimal Engineering System Inc.), receiving its trigger from the delay generator. For the studies reported here, a sonic jet (air, 200 psi stagnation pressure for Case I to V, 100 psi stagnation pressure for Case VI to VIII and ambient stagnation temperature) is injected into the test section through the 3 mm diameter hole in the tunnel wall or splitter plate resulting in a flow disturbance/blockage and an overall increase in flow pressure and temperature.

III. Results

The time sequential flow features induced by mass injection for Cases I - IV (described in Fig. 2) are depicted in Figs. 5 and 6. These cases are referred to as "asymmetric" boundary layer conditions. As mentioned above, the primary distinction between these flow conditions is the presence of either relatively thick boundary layers (Case I and III) or thin boundary layers (Case II and IV) on the model inlet wall through which the jet is injected. These conditions are also distinguished by the presence of a reflection shock due to the wedged inlet wall (Case II and III). By comparing these flow conditions, we see that the presence of relatively thick boundary layer has significant role in prompting the formation of the unstart shock.

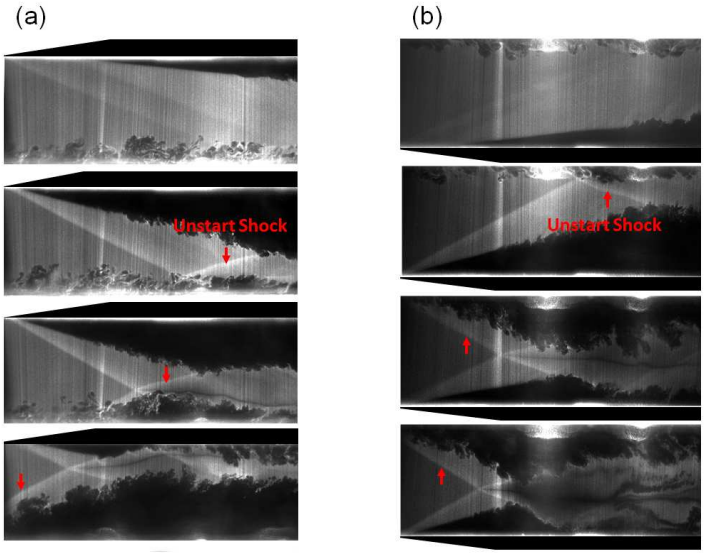

Figure 5. Time sequential PLRS images of unstart with: (a) Case I, and (b) Case IV flow configuration.

The image regions in Figs. 5 and 6 is 50 mm in length (along the streamwise direction starting at the lip of the model inlet) and 18.5 mm in height. The typical unstart induced by mass injection for Case I is shown in Fig. 5 (a). The boundary layer growth and separation on the bottom wall of the model inlet, initiated by mass injection, propagates upstream and generates an oblique (unstart) shock and the model inlet flow unstarts upon the arrival of

this oblique shock past the tip of the model inlet. During this unstart event, we also see a separated flow on the upper wall that also propagates upstream and produces a separation shock but this shock seems to anchor to the lip of the model inlet. The unstart dynamics for Case IV (but with the jet injected through the thin boundary layer) appear to be very similar (but inverted vertically) to that of Case I, as seen in Fig. 5 (b). The growth and separation of the boundary layer on the lower wall (jet injection wall) of model is observed as before. However, to our surprise, the separation shock again anchors at the lip of the model inlet. An oblique unstart shock appears on the upper wall where the relatively thick boundary layer resides. This unstart shock propagates upstream of the model inlet and unstarts the flow. By comparing Case I and IV, we see that the formation of the oblique unstart shock is favors the relatively thick boundary layer side, and is independent of the side in which the jet is injected.

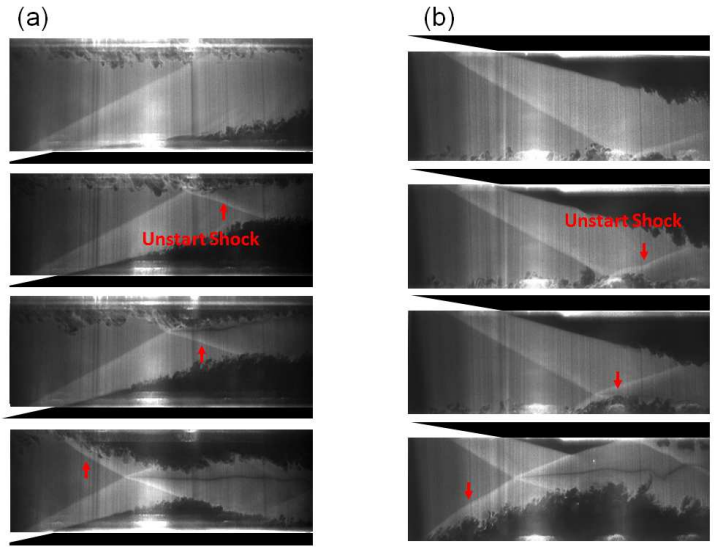

Figure 6. Time sequential PLRS images of unstart with: (a) Case II, and (b) Case III flow configuration.

The unstart dynamics induced by mass injection for Cases II (jet through thin boundary layer) and III (jet through thick boundary layer) with the presence of an incident oblique shock are depicted in Fig. 6 (a) and (b), respectively. Again, we see that the boundary layer growth and separation on the relatively thin boundary layer side (lower wall for Case II and upper wall for Case III) propagate upstream and spawn separation shocks that anchor on the lip of the model while disturbances on the relatively thick boundary layer side (upper wall for Case II and lower wall for Case III) spawn oblique unstart shocks. In general, we see little difference between the cases with and without this incident shock (i.e., between Fig. 5 and 6), however, it is noteworthy that the time to unstart (unstart duration) for Case I and IV is about 20 ms whereas for Case II and III it is around 25 ms. This delay in unstart when the incident shock is present is attributed to the favorable pressure rise generated near the shock reflection point.

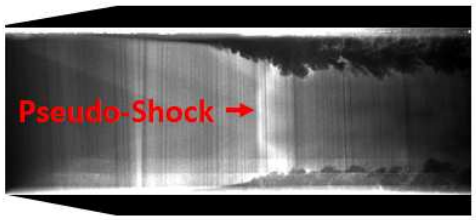

Figure 7. PLRS images of unstart with Case V flow configuration.

The Case V unstart dynamics is found to be very different than that of Cases I – IV. The oblique unstart shock that was seen in these asymmetric boundary layer model inlet flows does not appear in Case V. Instead, during unstart, we observe a coalescence of compression waves, i.e., a pseudo-shock, near the region of boundary layer separation, as depicted in Fig. 7. Such pseudo-shocks are often observed during the decelerating of supersonic flow in a duct.[31] We find that this pseudo-shock has a quasi-stationary mode, anchoring between the jet and the lip of the splitter plates for about 30 ms, resulting in a significant increase in the unstart time.

These studies indicate that the unstart dynamics is controlled by the boundary layer conditions. In particular, the delay (albeit slight) introduced by the presence of the incident shock, and the delay to unstart as a result of the thinning of the boundary layers (Case V) motivated the use of boundary layer actuation as a means of controlling unstart delay. In a recent study[26], we demonstrated the thinning and regularization of a thick supersonic turbulent

boundary layer by spanwise DBD forcing. Below, we describe initial results related to the delay of unstart by DBD actuation.

The unstart dynamics for Case VI (symmetric boundary layer), Case VII (asymmetric boundary layer due to tripping), and Case VIII (boundary layer tripping with actuation) are illustrated in Figs. 8, 9, and 10, respectively. The right images in these figures represent the planar Rayleigh scattering visualizations in the region in the vicinity of the jet whereas the left frames illuminate the upstream region near the splitter plate lips. In all cases, the imaging laser sheet is aligned with the edge of the exposed electrode (see Fig. 4). The Case VI configuration has identical boundary layer conditions to that of Case V except the channel height is reduced slightly (18.5 mm for Case V, 15 mm for Case VI). This reduction in height has little effect on the overall unstart dynamics and the flow features seen in Fig. 8 resemble those seen for Case V. Boundary layer growth and separation is observed on both the upper and lower walls of the model inlet following jet injection. Symmetric oblique shockwaves initiated near the jet region eventually merge into the pseudo-shock as the pressure disturbances propagate upstream. This pseudo shock appears to be quasi-stationary for approximately 10 ms and then eventually breaks down as the pressure rises, eventually unstarting the inlet when it arrives at the model entrance.

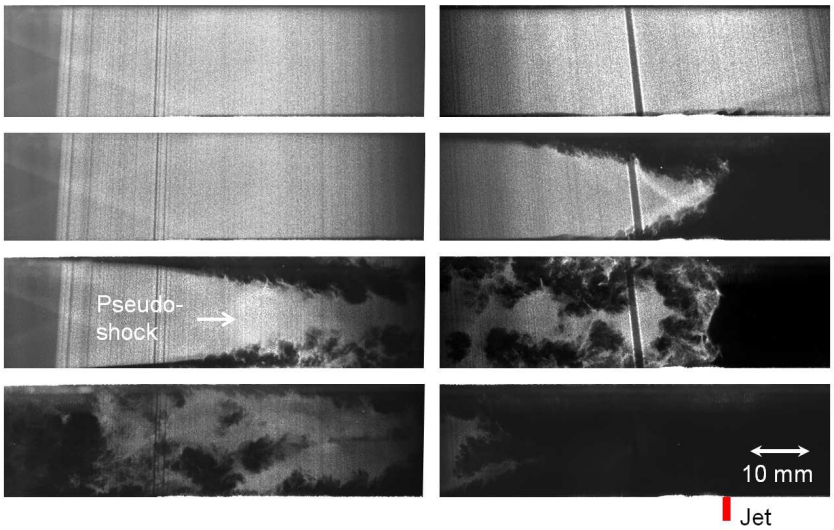

Figure 8. Time sequential unstart PLRS images in the Case VI flow configuration.

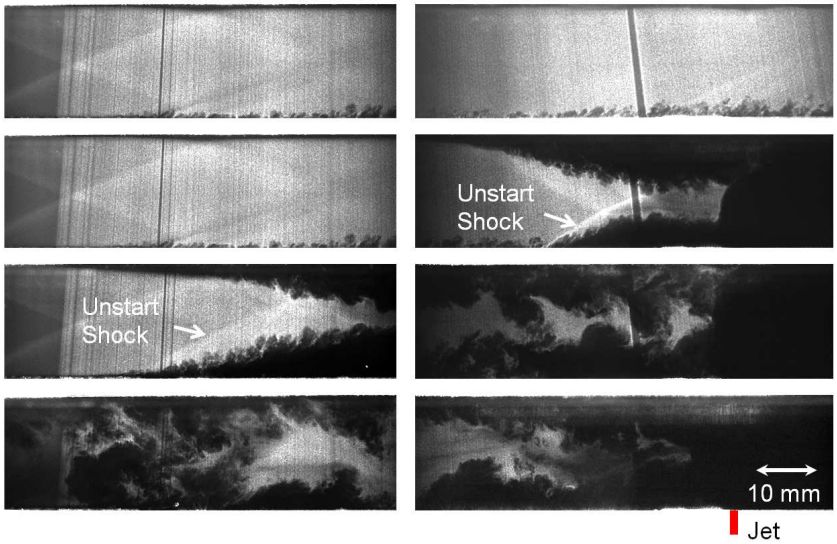

Figure 9. Time sequential unstart PLRS images in the Case VII flow configuration.

In Case VII, the boundary layer on the lower wall is tripped to provide an asymmetric boundary layer condition. As a result of tripping, a relatively thick boundary layer is seen to form on lower side of model inlet flow (see Fig. 9). A pseudo-shock does not appear in this case as a result of the breaking of the otherwise

symmetry condition. Instead, an oblique unstart shock spawned by the boundary layer growth and separation on the thicker boundary side propagates upstream and unstarts the flow. This oblique unstart shock does not experience a quasi-stationary regime so the duration of the unstart process for Case VII is much shorter than that of Case VI.

The results with DBD actuation on the tripped side of Case VII, i.e., Case VIII, are depicted in Fig. 10. One feature of this flow is that DBD actuation thins the boundary layer significantly on the wall that is tripped (lower wall). The effectiveness of the actuation persists for about 5 cm, when comparing the top images of Fig. 9 to that of Fig. 10. While an oblique shock appears to form initially as a result of the loss of actuator effectiveness near the point of jet injection, the shocks do eventually merge to form what appears to be a pseudo-shock and the flow resembles that of Case VI. This unstart pseudo shock has a quasi-stationary regime but it is relatively short, approximately 3 ms. We believe that more distributed discharge actuation and higher power can extend this regime.

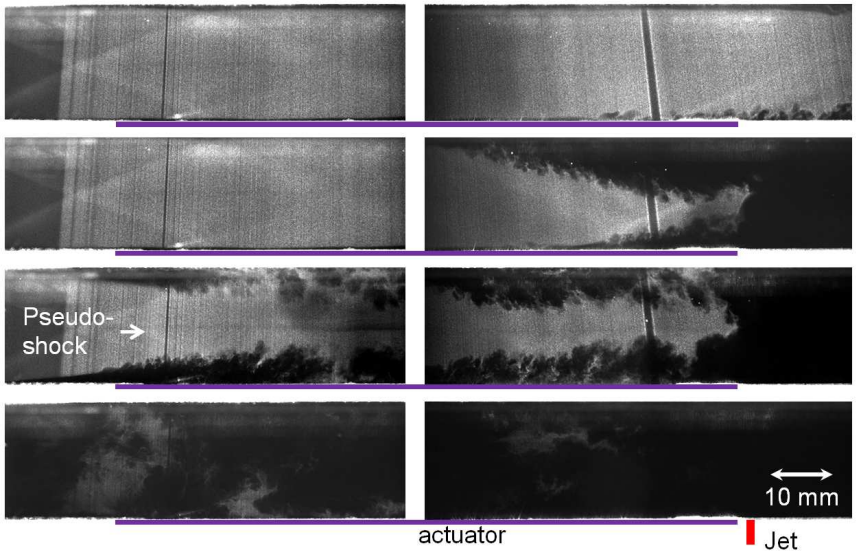

Figure 10. Time sequential unstart PLRS images in the Case VIII flow configuration.

The streamwise boundary layer velocity profiles measured using a pitot probe 10 mm upstream of the jet (on the jet wall side) for Case VI - VIII are shown in Fig. 11. The boundary layer thickness for the untripped Case VI condition is approximately 0.5 mm. The tripped Case VII configuration results in a boundary layer that is much thicker (about 2 mm) at this same location. This thicker boundary layer is the main reason for the differences in the unstart dynamics seen in Fig. 8 and 9. The plasma actuation (Case VIII) reduces the boundary layer thickness to around 1 mm. However, we see that this actuation could not completely reduce the thickness to that seen for the untripped case. The reduction in boundary layer thickness by DBD actuation is consistent with the transition from oblique to pseudo-shock cases seen when comparing Figs. 8 – 10.

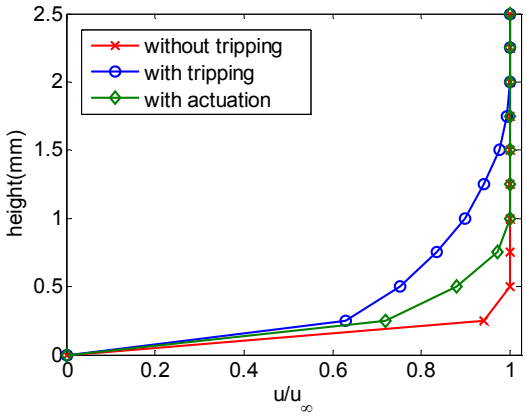

Figure 11. Freestream velocity profile.

The unstart duration provides a quantitative measure of how effective DBD actuation is on unstart. Experimentally, we define the unstart time (or duration) as the time interval between the jet injection is initially triggered (producing disturbances) and an abrupt pressure rise is measured on a pressure sensor located on the lower wind tunnel wall just downstream of the model entrance (see Fig. 12). Fig. 12 depicts a cartoon of the flow conditions outside of the model inlet before (Fig. 12 (a)) and after (Fig. 12 (b)) unstart. Figure 12 (c) is an actual experimental trace of the jet trigger signal, and the pressure sensor signal. We see that an abrupt pressure rise is detected at the sensor at a time delay Δt, when the unstart shock propagates beyond the model inlet.

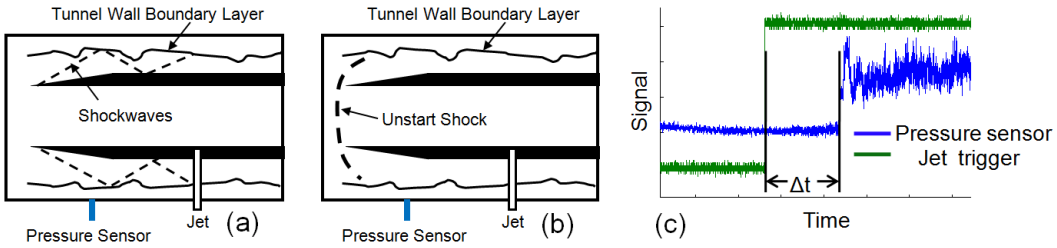

Figure 12. Schematic of flow conditions: (a) before unstart, (b) after unstart, and (c) definition of time to unstart, Δt.

Probability distribution functions (PDFs) of this unstart delay time are generated by more than one hundred unstart experiments for each of the three flow conditions (Case VI to VIII). These three PDFs are shown in Fig. 13. These are represented as corresponding histograms and as well as superimposed Gaussian fits. The blue, green and red color illustrate the unstart time PDFs for Cases VI, VII and VIII, respectively. The difference between the mean values for Case VI and VII is approximately 11.5 ms (due to the existence of a pseudo-shock for Case VII and its stationary regime). We see that DBD actuation delays unstart by about 2.5 ms. Although slight, it does represent an approximately 22% reduction in delay time between cases VI and VII. This delay is attributed to the thinning of the boundary layer and the transport of high speed free-stream fluid into the boundary layer, helping to overcome adverse pressure gradients generated by boundary layer separation.

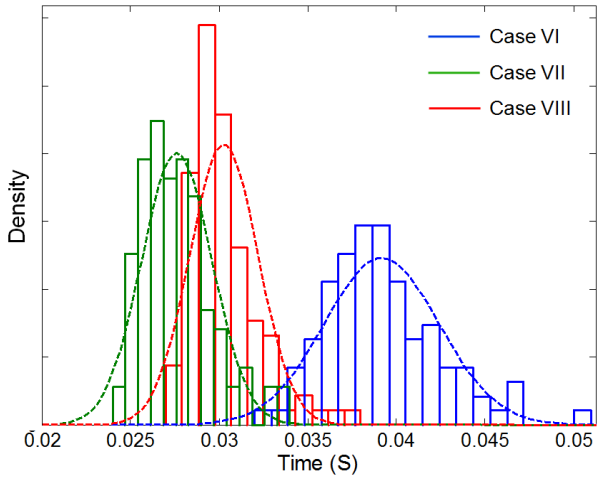

Figure 13. Unstart time distribution histogram and gaussian fit.

IV. Conclusion

Inlet unstart induced by mass injection was investigated for five different inlet flow configurations. Planar Laser Rayleigh Scattering imaging was used to visualize flow features during the unstart dynamics. It was found that unstart flow features (shock structure and time to unstart) are strongly affected by the initial boundary layer conditions prior to jet injection. In the presence of relatively thick boundary layers as a result of using the tunnel wall as one wall of the model inlet (asymmetric condition, Cases I - IV), oblique unstart shocks are spawned on the relatively thick boundary layer side, eventually propagating to the model entrance and unstarting the flow. This unstart characteristic was independent of the side in which the jet was injected and also relatively independent of the presence of a shock reflection due to the presence of an oblique incident shock. For these asymmetric boundary layer cases, the unstart time was found to be approximately 20 ms. With symmetric boundary layer conditions (Case V), an oblique unstart shock did not form. Instead, the symmetric cases led to the formation of a pseudo-shock which propagated upstream towards the model entrance, but which also had a quasi-stationary regime lasting for about 30 ms. The time to unstart in this case was approximately 55 ms. These results suggest that the unstart dynamics can be affected by boundary layer actuation and control.

The use of DBD actuation for controlling unstart was also investigated. Three additional flow conditions (Cases VI- VIII) were examined, under which the model inlet flow was isolated from the thicker boundary layers of the tunnel walls (as in Case V). The Case VI flow configuration was similar to that of Case V (Cases VI-VIII had a channel height that was slightly smaller) and generally similar flow dynamics were observed. Case VI resulted in the formation of a pseudo-shock that had a quasi-stationary regime that lasted 10 ms. Case VII differed in that one wall of the model inlet was tripped to be turbulent and this gave rise to a strong oblique unstart shock. The absence of a quasi-stationary pseudo-shock resulted in Case VII having a much shorter unstart time. With DBD actuation of this tripped turbulent boundary layer (Case VIII), the shock structure was transformed to that of a pseudo-shock with a quasi-stationary regime lasting 2.5 ms in duration. PDFs of unstart times provided clear indication of the benefits associated with DBD actuation but further enhancements in plasma forcing will be necessary to achieve conditions similar to those in the absence of turbulent boundary layers.

Acknowledgments

This research is supported in part by the Stanford Predictive Science Academic Alliance Program, which is funded by the Department of Energy (National Nuclear Security Administration) under Award Number DE-FC52-08NA28614.

References

[1]Emami, S., Trexler, C. A., Auslender, A. H., and Weidner, J. P., "Experimental investigation of inlet-combustor isolators for a dual-mode scramjet at a Mach number of 4," NASA Technical Paper 3502, 1995.

[2]Wieting, A. R., "Exploratory study of transient unstart phenomena in a three-dimensional fixed-geometry scramjet engine," NASA TN D-8156, 1976.

[3]Rodi, P. E., Emami, S., and Trexler, C. A., "Unsteady Pressure Behavior in a Ramjet/scramjet Inlet," *Journal of Propulsion and Powe*r, Vol. 12, No. 3, 1996, pp. 486-493.

[4]Shimura T., Mitani T., Sakuranaka N., and Izumikawa M., "Load Oscillations Caused by Unstart of Hypersonic Wind Tunnels and Engines," *Journal of Propulsion and Power*, Vol. 14, No. 3, 1998, pp. 348-353.

[5]O'Byrne, S., Doolan, M., Olsen, S. R., and Houwing, A. F. P., "Analysis of Transient Thermal Choking Processes in a Model Scramjet Engine," Journal of Propulsion and Power, Vol. 16, No. 5, 2000, pp. 808-814.

[6]Graham R. H., *SR-71 Blackbird*, MBI Publishing Company, St. Paul, MN, 2002, pp. 27-28.

[7]Mashio, S., Kurashina, K., Bamba, T., Okimoto, S., and Kaji, S., "Unstart Phenomenon Due to Thermal Choke in Scramjet Module," *AIAA/NAL-NASDA-ISAS 10th International Space Planes and Hypersonic Systems and Technologies Conference*, 2001, AIAA 2001-1887.

[8]Kodera, M., Tomioka, S., Kanda, T., Mitani, T., and Kobayashi, K. "Mach 6 Test of a Scramjet Engine with Boundary-Layer Bleeding and Two-Staged Fuel Injection," *12th AIAA International Space Planes and Hypersonic Systems and Technologies*, 2003, AIAA 2003-7049.

[9]Heiser, W. H. and Pratt, D. T., "Hypersonic air breathing propulsion," *AIAA Education Series*, 1993.

[10]McDaniel, K. S. and Edwards, J. R., "Three-Dimensional Simulation of Thermal Choking in a Model Scramjet Combustor," *39th Aerospace Sciences Meeting and Exhibit*, 2001, AIAA 2001-0382.

[11]Wagner, J. L., Yuceil, K. B., Valdivia, A., Clemens, N. T., and Dolling, D. S., "Experimental Investigation of Unstart in an Inlet/isolator Model in Mach 5 Flow,"AIAA Journal, Vol. 47, No. 6, 2009, pp. 1528-1542.

[12]Do, H., Im, S. Mungal, M. G., and Cappelli, M. A., "Visualizing Supersonic Inlet Duct Unstart Induced by Jet Injection using Rayleigh Scattering from Condensed CO_2," *Experiments in Fluids*, Vol. 50, 2010, pp. 1651-1657.

[13]Do, H., Im, S. Mungal, M. G., and Cappelli, M. A., "The Influence of Boundary Layers on Supersonic Inlet Flow Unstart Induced by Mass Injection," *Experiments in Fluids*, Vol. 51, 2011, pp 679-691.

[14]Curran, E. T., Heiser, W. H., and Pratt, D. T., "Fluid Phenomena in Scramjet Combustion Systems," *Annual Review of Fluid Mechanics,* Vol. 28, 1996, pp 332-360.

[15]Wang, X., and Le, J., "Computations of Inlet/Isolator for Scramjet Engine," *Journal of Thermal Science*, Vol. 9, 2000, pp. 334-338.

[16]Post, M. L., and Corke, T. C., "Separation Control on High Angle of Attack Airfoil Using Plasma Actuators," *AIAA Journal*. Vol.42, No. 11, 2004, pp. 2177-2184.

[17]Huang, J., Corke, T. C., and Thomas, F. O., "Unsteady Plasma Actuators for Separation Control of Low-Pressure Turbine Blades," *AIAA Journal*. Vol. 44, No. 7, 2006, pp. 1477-1487.

[18]Sung, Y., Kim,W., Mungal, M. G., and Cappelli, M. A., "Aerodynamic Modification of Flow Over Bluff Objects by Plasma Actuation," *Experiments in Fluids*, Vol. 42, No. 3, 2006, pp. 479-486.

[19]Do, H., Kim, W., Mungal, M. G., and Cappelli, M.A., "Bluff Body Flow Separation Control using Surface Dielectric Barrier Discharges," *45th AIAA Aerospace Sciences Meeting and Exhibit*, 2007, AIAA 2007-939.

[20]Grundmann, S., and Tropea, C., "Experimental Transition Delay Using Glow-Discharge Plasma Actuators," *Experiments in Fluids*, Vol. 42, No. 4, 2007, pp. 653-657.
[21]Porter, C. O., Baughn, J. W., McLaughlin, T. E., Enloe, C. L., and Font, G. I., "Plasma Actuator Force Measurements," *AIAA Journal*. Vol. 45, No. 7, 2007, pp. 1562-1570.
[22]Schatzman, D. M., and Thomas, F. O., "Turbulent Boundary Layer Separation Control Using Plasma Actuators," *4th Flow Control Conference*, 2008, AIAA 2008-4199.
[23]Jukes T. N., and Choi K-S., "Dielectric-Barrier-Discharge Vortex Generators: Characterisation and Optimisation for Flow Separation Control," *Experiments in Fluids*, Vol. 52, 2012, pp. 329-345.
[24]Roth, J. R., Sherman, D. M., and Wilkinson, S. P., "Boundary Layer Flow Control with a One Atmosphere Uniform Glow Discharge Surface Plasma," *36th AIAA Sciences Meeting and Exhibit*, 1998, AIAA 1998-0328.
[25]Moreau, E., "Airflow Control by Non-Thermal Plasma Actuators," *Journal of Physics D: Applied Physics*, Vol. 40, No. 3, 2007, pp. 605-636.
[26]Im, S., Do, H., and Cappelli, M. A., "Dielectric Barrier Discharge Control of a Turbulent Boundary Layer in a Supersonic Flow," Applied Physics Letters, Vol. 97, 2010, pp. 041503.
[27]Narayanaswamy, V., Raja, L. L., and Clemens, N. T., "Characterization of a High-Frequency Pulsed-Plasma Jet Actuator for Supersonic Flow Control," *AIAA Journal*. Vol. 48, No. 2, 2010, pp. 297-305.
[28]Leonov, S., Bityurin, V., Savischenko, N., Yuriev, A., and Gromov, V., "Influence of Surface Electrical Discharge on Friction of Plate in Subsonic and Transonic Airflow," *39th AIAA Aerospace Sciences Meeting and Exhibit*, 2001, AIAA 2001-640.
[29]Miles, R. B., and Lempert, W. R., "Quantitative flow visualization in unseeded flows," *Annual Review of Fluid Mechanics*, Vol. 29, 1997, pp. 285-326.
[30]Wu, P., Lempert, W. R., and Miles, R. B., "Megahertz Pulse-Burst Laser and Visualization of Shock-Wave/Boundary-Layer Interaction," *AIAA Journal*, Vol. 38, No. 4, 2000, pp. 672 – 679.
[31]Arai, T., Sugiyama, H., Abe, F., Takahashi, T., and Onodera, O., "Internal Structure of Pseudo-shock Waves in a Square Duct," *AIP Conference Proceeding*, Vol. 208, 1990, pp. 850-855.